

Investigation on the Faulty State of DFIG in a Microgrid

Minyou Chen, *Member, IEEE*, Lei Yu, Neal S. Wade, Xiaoqin Liu, Qing Liu, and Fan Yang

Abstract—Different faulty states of a doubly fed induction generator (DFIG) connected to a microgrid are investigated in this paper. First, the simulation model consisting of two DFIGs connected to IEEE 34-bus test feeder for two vector control based was set up to investigate the transient performance of the microgrid. Then, different types of faults of the DFIGs, including partial loss of excitation (PLOE), complete loss of excitation (CLOE), and interturn short circuit (ISC) were analyzed through the simulation model using vector control strategy. The experimental results indicate that the active power will increase during the PLOE, and the average increase of the amplitude is about 26%, which will decrease the electromagnetic torque by 8% and increase the voltage at the neighbor node, the stability of the microgrid will be broken eventually. For the CLOE, the active power decreases about 80%, and node voltage decreases by 9.4% due to the inverse absorption of the reactive power. When the ISC occurs, the average node voltage and the active power decrease together. Finally, the suggestion for the detection of the DFIG faults is presented, which could be helpful to protect the DFIG from fault accident.

Index Terms—Doubly fed induction generator (DFIG), fault analysis, loss of excitation, microgrid, vector control.

I. INTRODUCTION

THE renewable energy is becoming more and more important for the development of the world, especially for the countries, which lacks of primary energy. With the increase of the electric power demand in China, the power grid keeps extending and many ultrahigh-voltage (UHV) transmission lines have been built, which can satisfy the increasing electric power demand. However, new problems for the expanding power grid rise up, such as the high operation cost, great difficulty in operation, which also decreases the reliability and stability of the power grid [1].

The studies on the renewable resource have promoted the rapid development of distributed generation (DG) technique, especially the development and construction of the microgrid. In general, a microgrid is composed of the DGs, energy storage units, energy transfer units, variable loads, and it can operate either in the grid-connected mode or the islanded mode [2], [3]. In the past few years, many new microgrid have been built in the west and north of China, and wind power is frequently used in these microgrids. The power supply problem has been solved; however, new problem rises up, such as the accident of the wind generation system, which usually affect the steady operation of the microgrid. Hence, it is necessary to study the faults state of the wind generation system and the influence on the microgrid.

The wind power is one of the DGs in a microgrid, and currently there are three main kinds of wind generators (WGs) are frequently used, including [4]: constant speed constant frequency squirrel cage induction generator (SCIG), variable speed constant frequency doubly fed induction generator (DFIG), and variable speed permanent-magnetic direct drive synchronous generation (PMSG). At present, the doubly fed wind generator is widely used because of its low capacity of the converter, relative simple control, in addition, it can operate in constant voltage or constant power factor mode [5].

Many studies on the control strategies of the microgrid have been carried out by some researchers, and great achievements have been obtained [6]–[9]. In order to ensure the stable operation of the microgrid, some researches about the fault and protection of microgrid have been done [10], [11]. In [12] and [13], the authors analyze the performance of the DFIG during the grid faults. Wind power is one of the main DG in a microgrid, therefore, it is necessary to study the failure characteristics of the DFIG and the impact of the microgrid.

In this paper, based on the control methods achieved by the current studies, the investigation of the faulty state of the DFIG in a microgrid is conducted and a detection suggestion for these faults is presented. First, the model for two vector-control-based DFIG was set up, then simulation to investigate the transient performance of two DFIGs connected to the IEEE 34-bus test feeder was carried out. Performance of the DFIGs with different fault was analyzed, including partial loss of excitation (PLOE), complete loss of excitation (CLOE), interturn short circuit (ISC) of the DFIG, and results indicate that the active power will increase during the PLOE, and the average increase of the amplitude is about 26%, which will result in the decreasing of the electromagnetic torque by 8% and the increase of the voltage at the neighbor node; finally, the stability of the microgrid will be broken. For the CLOE, the active power decreases about 80%, and node voltage decreases by 9.4% due to the inverse absorption

Manuscript received July 1, 2010; revised August 20, 2010; accepted November 6, 2010. Date of current version August 5, 2011. This work was supported by the National Science Foundation of China under Grant 50910234 and the National “111” Project of China under Grant B08036. Recommended for publication by Associate Editor J. M. Guerrero.

M. Chen, L. Yu, and F. Yang are with State Key Laboratory of Power Transmission Equipment and System Security and New Technology, Chongqing University, Chongqing 400044, China.

N. S. Wade is with School of Engineering, University of Durham, Durham DH1 1TA, U.K.

X. Liu is with Chongqing Nanping Power Supply Bureau, Chongqing 400066, China.

Q. Liu is with Chongqing Power Grid Maintenance Company, Chongqing 400015, China.

Color versions of one or more of the figures in this paper are available online at <http://ieeexplore.ieee.org>.

Digital Object Identifier 10.1109/TPEL.2010.2094626

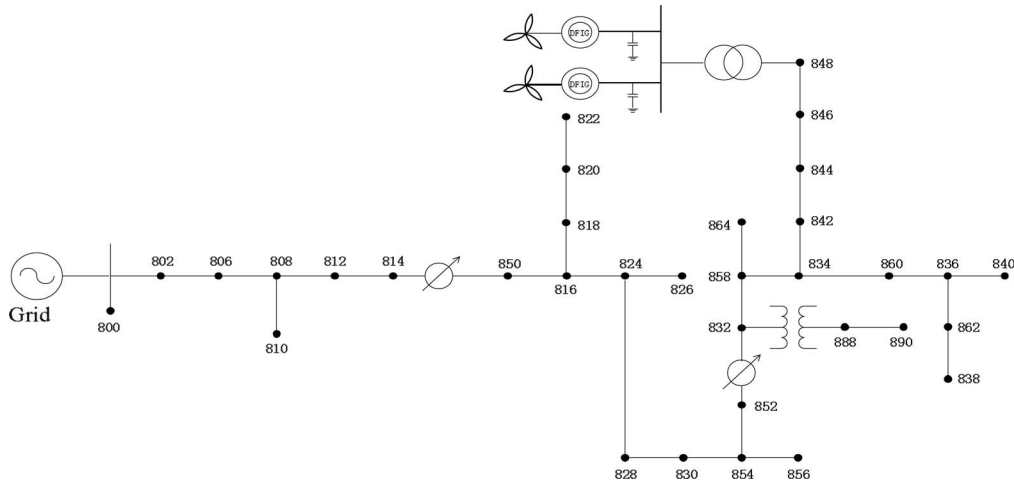


Fig. 1. One-line diagram of 34-bus test feeder system with two DFIGs.

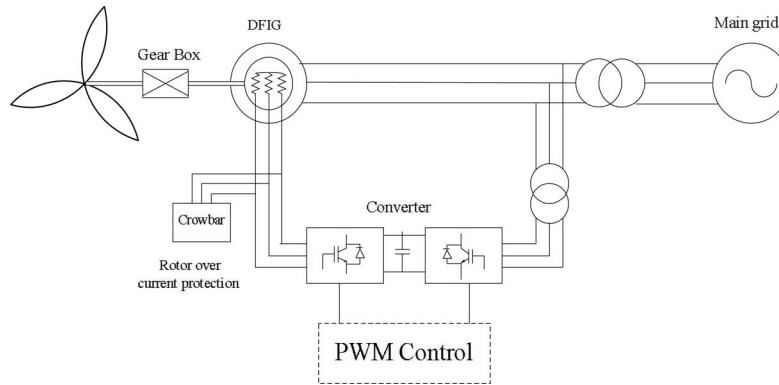


Fig. 2. Basic configuration of DFIG connected to the grid.

of the reactive power, in this case, reactive power compensation must be available to make sure the steady of the microgrid. When the ISC occurs, the average node voltage and the active power decrease together. In the end, suggestion for the detection of the fault mentioned in the paper is presented, which can help to avoid the damage caused by the fault of the DFIG.

The remaining parts of the paper are arranged as follows. Section II describes the structure of the microgrid and presents the simulation model; the control method for the DFIG is presented in Section III, results are analyzed and a fault detection scheme is discussed in Section IV, and finally, the conclusions come at Section V.

II. SIMULATION MODEL SETUP

To study the change of the parameters of a microgrid and the faulty state of the DFIGs, the microgrid model shown in Fig. 1 is set up, which is composed of one-line diagram of the test feeder and two DFIGs. On IEEE 34-bus test feeder, there is a small 4.16 kV section in the 24.9 kV feeders, and there are two-line voltage regulators to support the voltage under normal circumstance. In order to simplify the model, the parameters of two DFIG are set as the same, the rated capacity is 2 MW and other parameters are as the same as those in [14]. The capacity of

the transformer in the model is 100 MVA, and its transformation ratio is 0.69/24.9 kV.

For the DFIG in the model shown in Fig. 1, it is composed of wind turbine, gearbox, induction machine, converter, and transformer, and Fig. 2 shows the schematic diagram of the DFIG. The basic structure of doubly fed machine is similar with an induction generator, but the rotor contains three-phase symmetrical excitation winding, and the converter provides a variable amplitude, frequency, and phase excitation current. The stator of DFIG is directly connected to the grid, and the rotor is connected to a back-to-back voltage-source converter to the grid with a crowbar, which is used as the rotor overcurrent protection [15]. The application of the pulsewidth modulation (PWM) technique can make the DFIG operate at a wide speed range, and the energy could be bidirectional to the grid.

III. VECTOR CONTROL FOR THE DFIG

The vector control for the DFIG is mainly based on the control of the grid and rotor-side four-quadrant insulated gate bipolar transistor (IGBT) converter. The main task for the grid-side converter is to maintain the dc capacitor voltage between two converters as a constant and ensure the stability of grid-side voltage, meanwhile, the main task for the rotor-side converter

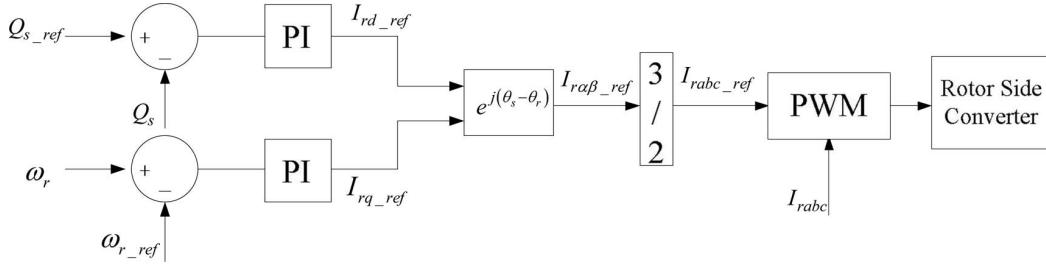


Fig. 3. Vector control configuration diagram for the rotor-side converter.

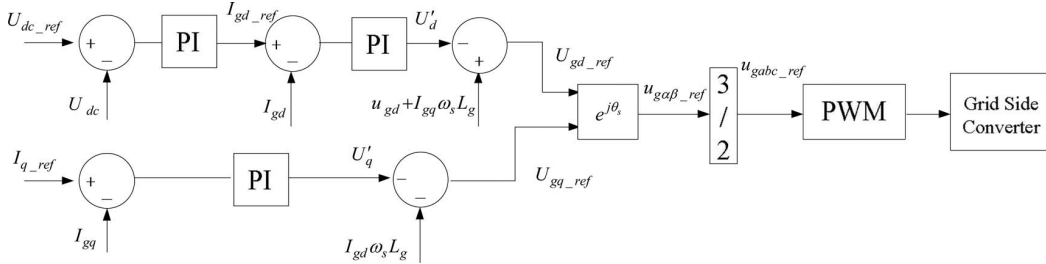


Fig. 4. Vector control frame of the grid-side PWM rectifier.

is to make the stator output active power tracking the desired value and keep the power factor constant [16], [17].

A. Rotor-Side PWM Vector Control

Since the stator is connected to the grid and the frequency can be considered as a constant and the influence of the stator winding resistance is small, hence the stator winding resistance can be ignored. The induction machine is controlled in a synchronous rotating d - q axis coordinate, in which the d -axis is along the stator-flux vector. Therefore, the stator voltage vector is along the q -axis. By ignoring the DFIG stator electromagnetic transient process, the active and reactive power at the stator terminal can be calculated as follows [18]:

$$\begin{aligned} P_s &= \frac{3}{2} u_{sq} i_{sq} = -\frac{3}{2} u_s \frac{L_m}{L_s} i_{rq} \\ Q_s &= \frac{3}{2} u_{sq} i_{sd} = \frac{3u_s}{2L_s} (\Psi_s - L_m i_{rd}) \end{aligned} \quad (1)$$

where P_s and Q_s are active and reactive power of stator winding, u_s is the DFIG phase voltage, and i_{rd} and i_{rq} are the component of rotor current along d - and q -axes, respectively. In the synchronous rotating coordinate

$$\begin{aligned} L_s &= L_{ls} + L_m \\ L_r &= L_{lr} + L_m \\ L_m &= \frac{3L_{sr}}{2} \end{aligned} \quad (2)$$

where L_{ls} and L_{lr} are the leakage inductance of stator and rotor and L_{sr} is the mutual inductance between the stator and the rotor.

According to (1), the active power P_s can be controlled by i_{rq} , and the reactive power Q_s can be controlled by i_{rd} . Because there is no interaction between i_{rq} and i_{rd} , therefore, Q_s would

not be changed when the i_{rq} is changed to control P_s . Fig. 3 is the schematic diagram of the vector control at the rotor side.

B. Grid-Side PWM Vector Control

The grid-side converter is controlled by the vector control program based on the grid voltage vector, and the decoupling control for the active and reactive power. The d -axis component of grid-side converter current is used to keep the dc bus voltage constant, and the q -axis component of grid-side converter current is used to control the reactive power transfer between grid-side converter and grid.

Therefore, the active and reactive power P_g and Q_g of grid-side converter can be calculated by

$$\begin{aligned} P_g &= \frac{3}{2} u_{gd} i_{gd} \\ Q_g &= -\frac{3}{2} u_{gd} i_{gq} \end{aligned} \quad (3)$$

where u_{gd} is the d -axis component of grid voltage vector, and i_{gd} and i_{gq} are the d - and q -axes component of grid-side converter current. The control of grid-side converter is mainly based on the control of its voltage, and need to establish the contact between converter voltage u_{gc} , and i_{gd} and i_{gq} . In the synchronous rotating coordinate, the grid-side voltage equation can be formulated as follows:

$$\begin{aligned} u_{gcd} &= u_{gd} + \omega_s L_g i_{gq} - \left(R_g i_{gd} + L_g \frac{di_{gd}}{dt} \right) \\ u_{gcq} &= -\omega_s L_g i_{gd} - \left(R_g i_{gq} + L_g \frac{di_{gq}}{dt} \right) \end{aligned} \quad (4)$$

where ω_s is the stator voltage angular velocity, and R_g and L_g are the induction winding resistance and inductance, respectively. Grid-side converter vector control structure diagram is illustrated in Fig. 4.

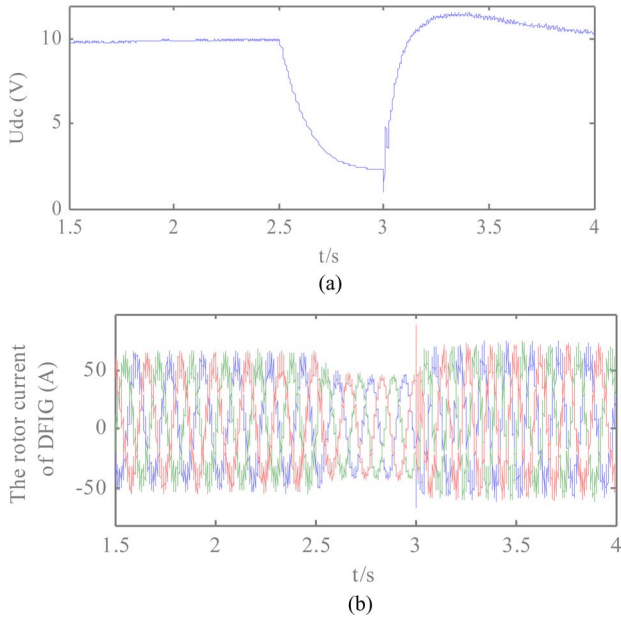


Fig. 5. DC voltage of converter and rotor current of DFIG. (a) DC voltage of converter U_{dc} . (b) Rotor current.

IV. SIMULATION AND RESULTS FOR THE FAULTY STATE OF THE DFIG

During the practical operation of the generator, faults may rise up because of the aging of power electronic devices, short circuited of the rotor winding, open circuit of the excitation winding, etc. For the normal operation, the generator can run at supersynchronous state or subsynchronous state [19]. Under the faulty state of a DFIG, the active power, reactive power, voltage, and current of generator stator will change. Therefore, in this part, the investigation on the change of the DFIG status is performed, such as the PLOE, CLOE, and ISC of the rotor winding exists in the DFIG. Then, a fault detection scheme is presented.

In the simulation, the DFIG model is operating at the power factor constant mode and the reactive power Q_{ref} is 0 kvar in the model, the wind speed is 10 m/s, and at the 2.5 s, the DFIG failure rise up. In order to facilitate the analysis, the failure duration was extended to 0.5 s. At the time of 3 s, the accident eliminated, and the impact of the reclosing to the system at the same time is simulated.

A. Result for PLOE

Because the grid-side converter is mainly used to maintain the dc voltage U_{dc} ; therefore, when the grid-side PWM control opened under the fault conditions, the dc bus in the grid side will lose the voltage support. But the excitation of generator will not disappeared completely; therefore, the generator will operate in the state of PLOE.

Before the fault, the generator runs at subsynchronous situation, and the grid-side converter absorbs power to stabilize the voltage of dc bus. After the accident, the grid-side converter disconnects from the grid, the rotor-side current is provided by the capacitor, and the change of the voltage U_{dc} is shown in

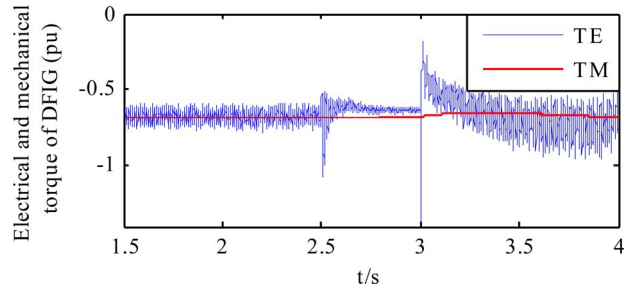


Fig. 6. Mechanical and electromagnetic torque of DFIG.

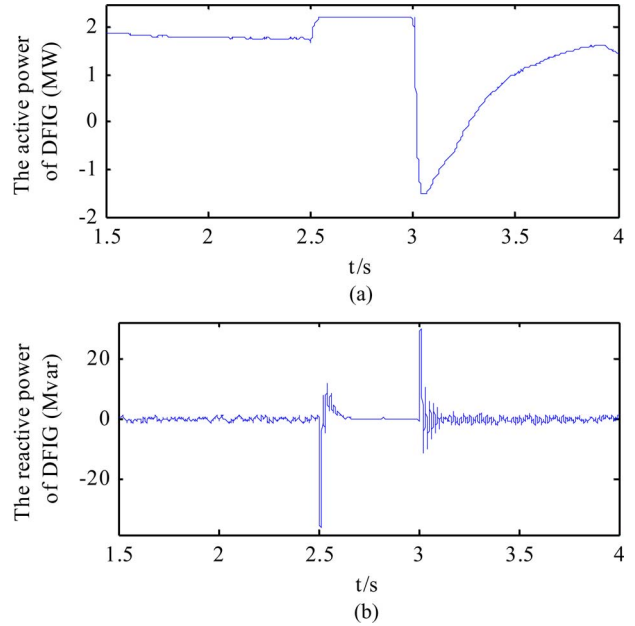


Fig. 7. Change of the active and reactive power of DFIG for PLOE. (a) Active power of DFIG. (b) Reactive power of DFIG.

Fig. 5(a). It is obvious that the U_{dc} decreases in the exponential form for 2.5 to 3 s, and the amplitude decreases from 10 to 2.2 V. Because the excitation current of rotor side is provided by the voltage-source converter; therefore, when the capacitor voltage U_{dc} decreases, the rotor current will decline, and the amplitude of three-phase current will also decrease in the exponential form from 67.5 to 41.7 A, as shown in Fig. 5(b).

At the same time, the torque imbalance will happen in the generator, i.e., the absolute value of the mechanical torque is greater than the electromagnetic torque, as shown in Fig. 6, and compared with the mechanical torque, the electromagnetic torque declines about 8%. The excessive torque will speed up the rotor, and the active power of generator temporarily increases, the amplitude of the difference can reach 26%, as shown in Fig. 7(a), which will result in the decreasing of the electromagnetic torque by 8% and the increase of the voltage at the neighbor node; finally, the stability of the microgrid will be broken. According to Fig. 7(b), the reactive power can be well controlled near the reference value because the DFIG operates at the reactive power constant mode of which the reference value is 0 var, but when the fault appear, the reactive power of machine will fluctuate. The voltage of node 846 has the greatest change for the

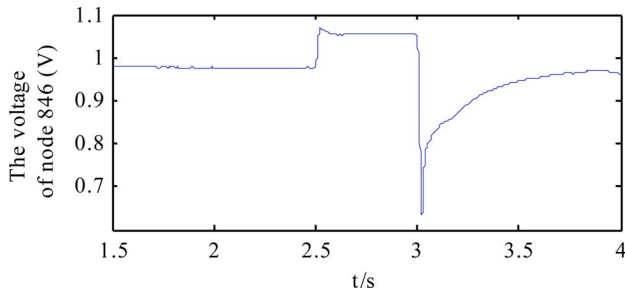


Fig. 8. Node voltage for PLOE.

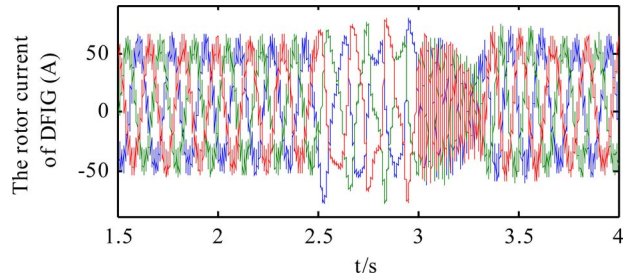


Fig. 9. Rotor current of DFIG for CLOE.

system in the fault state, and the per unit value of voltage rose by 8.3%, as shown in Fig. 8. After the accident, the grid side of DFIG reconnects to the grid, then the active and reactive power fluctuates violently.

Therefore, the PLOE of the DFIG can result in the instant pulse to the microgrid, to avoid the power accident in the microgrid, some monitoring measure should be adopted.

B. Result for CLOE

When the three-phase winding short circuit of the DFIG happens because of the fault of the rotor-side converter or slip ring, the rotor may lose the excitation and the CLOE may rise up [20]. Here, the analysis on the state of the generator of CLOE is presented.

The simulation result for the rotor current of the DFIG is shown in Fig. 9, its amplitude will not reduce to zero suddenly, because there exists the equivalent inductance. During the fault, the current lost nearly five waveforms. After the winding short, the rotor will form a loop; at this time, the DFIG changes into an induction wind generator. Therefore, the generator will absorb inductive reactive power from the grid to maintain air gap magnetic field. As shown in Fig. 10(a), 19.2 Mvar reactive power is need to meet the running demand. Fig. 10(b) indicates that after reestablishing the magnetic field, the DFIG continues to output active power. This makes it possible for the fault recovery and the operation reliability of generators will be improved. It is obvious that the amplitude of the active power substantially reduced when it operates in the asynchronous state, the output active power is only about 20% of rated value.

Because the generator absorbs reactive power from the grid, the grid voltage will change. The investigated result of the node voltage change of the grid is shown in Fig. 11. It can be seen that the average difference between the normal node voltage of 846

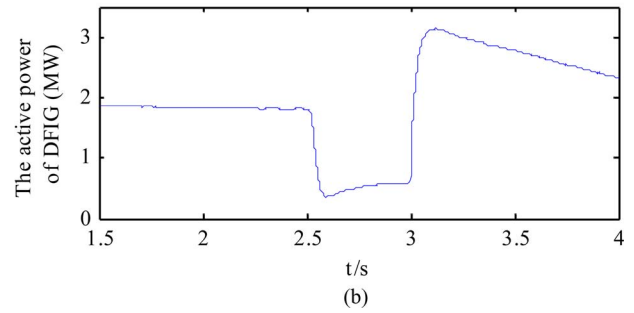
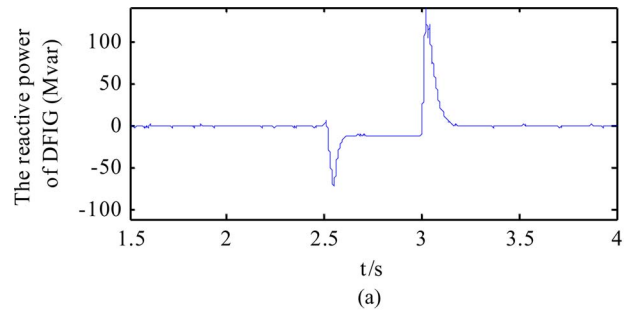


Fig. 10. Active and reactive power of DFIG for CLOE. (a) Reactive power of DFIG. (b) Active power of DFIG.

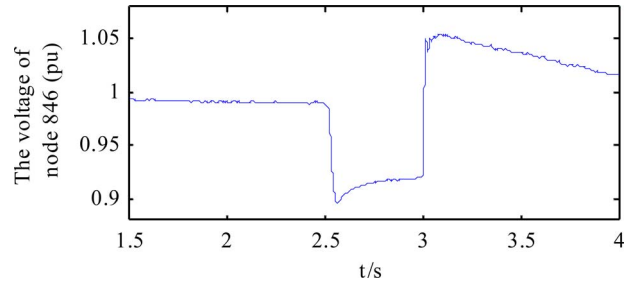


Fig. 11. Node voltage of 846 for CLOE.

and the faulty voltage can reach 9.4% of the normal value when the penetration rate of DFIG is low, which can influence the stability of the microgrid. Therefore, the corresponding measures should be taken to eliminate the impulse on the microgrid.

C. Result for ISC Fault

The ISC fault usually occurs in the DFIG in the case of long time running and high environmental temperature. When the short circuit of the rotor winding happens, the terminal voltage of the generator will change with the reduction of the effective turns ratio (shown in Table I), and the change amplitude depends on the count of the short-circuit winding. The following is the simulation result when different turn of short-circuit winding exists in the rotor winding.

The change of the active power and node voltage are shown in Fig. 12, zero point is in the normal state, the rotor effective turn decreases with the increase of the short-circuit rotor windings, the active power and average node voltage will decrease. When 10% of the rotor winding is short circuit, the difference of the active power can reach 35%, while the difference of the voltage only reaches 3%.

TABLE I
RELATIONSHIP BETWEEN TERMINAL VOLTAGE AND THE ROTOR TURNS

Rotor Turns Decline Rate (%)	0	2	4	6	7	10
Effective Turns Ratio	2.6377	2.5849	2.5322	2.4794	2.4267	2.3739
Terminal Voltage (<i>p.u</i>)	1.0403	1.0329	1.0311	1.0247	1.0171	1.0101

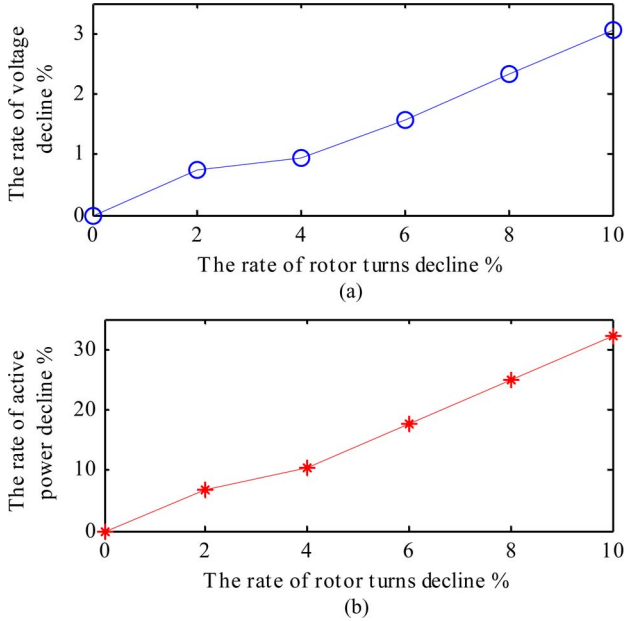


Fig. 12. Relationship between active power and node voltage and the rotor turns.

D. Analysis on the Fault Detection of the WGs Fault

According to the simulation results, the fluctuation of the system voltage, the active and reactive power of DFIG will emerge when the accident happens, what is worse, damage maybe caused to other devices in the microgrid; therefore, it is necessary to detect such fault in advance. Therefore, in this part, suggestion for the detection of the fault of a DFIG is presented, and Fig. 13 shows the schematic diagram.

In Fig. 13, a voltage sensor is used to measure the dc voltage of the converter, which can be used to check the fault of PLOE. A reactive power meter is used to measure the reactive power on the terminal of the DFIG, and another voltage sensor is installed to measure the terminal voltage of the DFIG, according to the measured reactive power and the terminal voltage, the fault of CLOE can be determined. To make an accurate detection on the fault, a self-organizing map (SOM) neural network can be used. In order to improve the classification accuracy of the SOM, simulated data and real failure data will be used to train the network. All the information of the input vector, which includes the fault characteristics, the rules of failures and the weigh coefficient, will be memorized, hence through the training of the network, the fault feature extraction also will be realized. In addition, with the input detection signals, the fault classification can be achieved.

The aforementioned is the suggestion for the fault detection of a DFIG, for the practical application of the fault de-

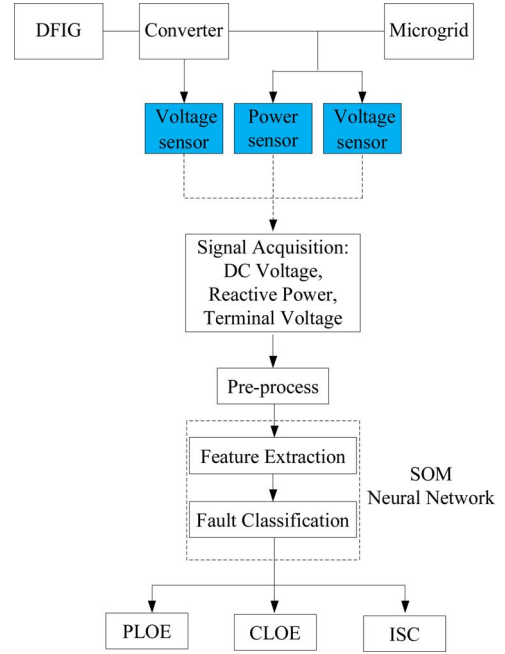


Fig. 13. Fault detection diagram.

tection system shown in Fig. 13, some filed tests should be performed.

V. CONCLUSION

In this paper, a vector control method for DFIG was presented, and the faults of loss of excitation were simulated when the DFIG was connected to the test system, then some qualitative analyses have been discussed. According to the simulation results, it can be concluded as follows.

- 1) The active power may temporarily increase when the DFIG in the PLOE fault and the node voltage of the system increases at the same time. After the fault, the active and reactive power fluctuates violently when the converter reconnects to the grid, which could result in the impulse on the microgrid.
- 2) For the CLOE fault, the machine is running into an asynchronous state, the active power will reduce and absorb reactive power, the voltage may decline. If the penetration rate of DFIG is low, the reactive power compensation is commanded to stabilize the voltage; if the penetration rate is high, WGs are advised to disconnect from the grid.
- 3) For the short circuit of the rotor winding, with the increase of the turn of the short-circuit rotor winding, the difference between the normal active power and average node voltage increases, and when 10% of the rotor winding is short

circuited, the difference of the active power is larger than the voltage's. Therefore, such type of the fault mainly has an effect on active power balance of the system.

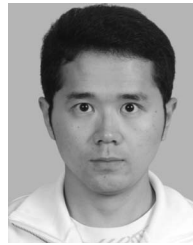
REFERENCES

- [1] C. Wang and P. Li, "Development and challenges of distributed generation, the micro-grid and smart distribution system," *Dianli Xitong Zidonghua/Autom. Electr. Power Syst.*, vol. 34, pp. 10–14, 2010.
- [2] A. Domijan, F. H. Torres, and C. A. Bel, "Microgrids: A look into the power delivery system of the future," in *Proc. 2007 9th IASTED Int. Conf. Power Energy Syst.*, 3–5 Jan., pp. 305–307.
- [3] B. Kroposki, T. Basso, and R. DeBlasio, "Microgrid standards and technologies," in *Proc. 2008 IEEE Power Energy Soc. 2008 Gen. Meeting: Convers. Del. Electr. Energy 21st Century*, 20–24 Jul., pp. 1–4.
- [4] M. S. A. Rapheal, V. G. Ram, V. K. Ramachandramurthy, and W. P. Hew, "Dynamic response of different wind generator topologies connected to medium size power grid," in *Proc. 2009 IEEE Bucharest PowerTech: Innovative Ideas Toward Electr. Grid Future*, 28 Jun.–2 Jul., pp. 1–6.
- [5] M. Shahabi, M. R. Haghifam, M. Mohamadian, and S. A. Nabavi-Niaki, "Microgrid dynamic performance improvement using a doubly fed induction wind generator," *IEEE Trans. Energy Convers.*, vol. 24, no. 1, pp. 137–145, Mar. 2009.
- [6] Y. W. Li, D. M. Vilathgamuwa, and P. C. Loh, "Robust control scheme for a microgrid with PFC capacitor connected," *IEEE Trans. Ind. Appl.*, vol. 43, no. 5, pp. 1172–1182, Sep./Oct. 2007.
- [7] J. M. Guerrero, J. C. Vasquez, J. Matas, M. Castilla, and L. Garcia de Vicuna, "Control strategy for flexible microgrid based on parallel line-interactive UPS systems," *IEEE Trans. Ind. Electron.*, vol. 56, no. 3, pp. 726–736, Mar. 2009.
- [8] A. L. Dimeas and N. D. Hatziargyriou, "Operation of a multiagent system for microgrid control," *IEEE Trans. Power Syst.*, vol. 20, no. 3, pp. 1447–1455, Aug. 2005.
- [9] E. Barklund, N. Pogaku, M. Prodanovic, C. Hernandez-Aramburo, and T. C. Green, "Energy management in autonomous microgrid using stability-constrained droop control of inverters," *IEEE Trans. Power Electron.*, vol. 23, no. 5, pp. 2346–2352, Sep. 2008.
- [10] E. Sortomme, S. S. Venkata, and J. Mitra, "Microgrid protection using communication-assisted digital relays," *IEEE Trans. Power Del.*, vol. 25, no. 4, pp. 2789–2796, Oct. 2010.
- [11] M. Bruccoli, T. C. Green, and J. D. F. McDonald, "Modelling and analysis of fault behaviour of inverter microgrids to aid future fault detection," in *Proc. 2007 IEEE Int. Conf. Syst. Syst. Eng.*, 16–18 Apr., pp. 1–6.
- [12] F. K. A. Lima, A. Luna, P. Rodriguez, E. H. Watanabe, and F. Blaabjerg, "Rotor voltage dynamics in the doubly fed induction generator during grid faults," *IEEE Trans. Power Electron.*, vol. 25, no. 1, pp. 118–130, Jan. 2010.
- [13] O. Anaya-Lara, X. Wu, P. Cartwright, J. B. Ekanayake, and N. Jenkins, "Performance of doubly fed induction generator (DFIG) during network faults," *Wind Eng.*, vol. 29, pp. 49–66, 2005.
- [14] P. Ledesma and J. Usaola, "Doubly fed induction generator model for transient stability analysis," *IEEE Trans. Energy Convers.*, vol. 20, no. 2, pp. 388–397, Jun. 2005.
- [15] Y. Liao, H. Li, J. Yao, and K. Zhuang, "Low voltage ride-through control strategy of a doubly fed induction generator wind turbine with series grid-side converter," *Zhongguo Dianji Gongcheng Xuebao/Proc. Chin. Soc. Electr. Eng.*, vol. 29, pp. 90–98, 2009.
- [16] L. Peng, Y. Li, J. Chai, and G. Yuan, "Vector control of a doubly fed induction generator for stand-alone shaft generator systems," *Qinghua Daxue Xuebao/J. Tsinghua Univ.*, vol. 49, pp. 938–942, 2009.
- [17] L. Shuhui and T. A. Haskew, "Analysis of decoupled d-q vector control in DFIG back-to-back PWM converter," in *Proc. 2007 IEEE Power Eng. Soc. Gen. Meeting*, 24–28 Jun., pp. 1–7.
- [18] S. Feng, H. Zhao, and W. Wang, "Studies on the variable speed wind turbine control system based on PSCAD/EMTDC," in *Proc. 2006 Int. Conf. Power Syst. Technol.*, 22–26 Oct., pp. 1–9.
- [19] Z. Kanjun, Y. Xianggen, C. Deshu, Z. Zhe, and C. Wei, "Simulation analysis of dynamic performance for hydro-generator under loss of excitation condition," in *Proc. 2006 41st Int. Univ. Power Eng. Conf.*, 6–8 Sep., pp. 540–544.
- [20] A. P. De Moraes, G. Cardoso, Jr., and L. Mariotto, "An innovative loss-of-excitation protection based on the fuzzy inference mechanism," *IEEE Trans. Power Del.*, vol. 25, no. 4, pp. 2197–2204, Oct. 2010.



Minyou Chen (M'05) was born in Chongqing, China. He received the M.Sc. degree from Chongqing University, Chongqing, in 1987, and the Ph.D. degree in control engineering from the University of Sheffield, Sheffield, U.K., in 1998.

He is currently a Professor at Chongqing University. He is the author or coauthor of more than 100 papers. His research interests include intelligent modeling and control, signal and image processing, state monitoring, and fault diagnosis in power systems.



Lei Yu was born in Hubei, China, in 1985. He received the M.S. degree in electrical engineering from Chongqing University, Chongqing, China, where he is currently working toward the Ph.D. degree in electrical engineering.

His research interests include the coordinated control for the microgrid.

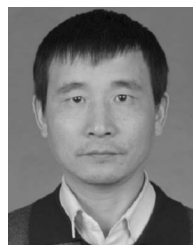
Neal S. Wade received the B.Sc. and Ph.D. degrees in electronic and electrical engineering from Glasgow University, Scotland, U.K., in 1997 and 2002, respectively.

He is currently a Research Associate in New and Renewable Energy Group, School of Engineering, University of Durham, Durham, U.K. His research interests include reliability of renewable energy conversion systems and energy storage control on electric distribution networks.



Xiaoqin Liu was born in 1973. She received the B.Sc. degree from the Department of Electrical Engineering, Chongqing Radio and TV University, Chongqing, China, and the M.Sc. degree from School of Electrical Engineering, Chongqing University, Chongqing, both in electrical engineering.

She is currently with Chongqing Nanping Power Supply Bureau, Chongqing, where she is engaged with the dispatching and operation of the power grid.



Qing Liu was born in Chongqing, China. He received the B.Sc. degree in electrical engineering from Chongqing Electric Power Institute, Chongqing, in 2002.

He is currently with the Chongqing Electric Power Overhaul Company, Chongqing.



Fan Yang was born in Shandong, China, in 1980. He received the Ph.D. degree in electrical engineering from Chongqing University, Chongqing, China, in 2008.

He is currently with State Key Laboratory of Power Transmission Equipment and System Security and New Technology, Chongqing University, Chongqing. His research interests include the intelligent calculation.